Molecular Biology of the Cell
Vol. 10, 4163–4176, December 1999

Synaptic Vesicles Form by Budding from Tubular Extensions of Sorting Endosomes in PC12 Cells

Heidi de Wit,* Yael Lichtenstein,† Hans J. Geuze,* Regis B. Kelly,† Peter van der Sluijs,* and Judith Klumperman*‡

*Department of Cell Biology, University Medical Centre and Institute for Biomembranes, Utrecht University, 3584 CX Utrecht, The Netherlands; and †Department of Biochemistry and Biophysics, Hormone Research Institute, University of California, San Francisco, California 94143-0534

Submitted June 4, 1999; Accepted September 8, 1999
Monitoring Editor: Suzanne R. Pfeffer

The putative role of sorting early endosomes (EEs) in synaptic-like microvesicle (SLMV) formation in the neuroendocrine PC12 cell line was investigated by quantitative immunoelectron microscopy. By BSA-gold internalization kinetics, four distinct endosomal subcompartments were distinguished: primary endocytic vesicles, EEs, late endosomes, and lysosomes. As in other cells, EEs consisted of vacuolar and tubulovesicular subdomains. The SLMV marker proteins synaptophysin and vesicle-associated membrane protein 2 (VAMP-2) localized to both the EE vacuoles and associated tubulovesicles. Quantitative analysis showed that the transferrin receptor and SLMV proteins colocalized to a significantly higher degree in primary endocytic vesicles then in EE-associated tubulovesicles. By incubating PC12 cells expressing T antigen-tagged VAMP (VAMP-TAg) with antibodies against the luminal TAg, the recycling pathway of SLMV proteins was directly visualized. At 15°C, internalized VAMP-TAg accumulated in the vacuolar domain of EEs. Upon rewarming to 37°C, the labeling shifted to the tubular part of EEs and to newly formed SLMVs. Our data delineate a pathway in which SLMV proteins together with transferrin receptor are delivered to EEs, where they are sorted into SLMVs and recycling vesicles, respectively.

INTRODUCTION

Synaptic vesicles (SVs) are specialized ~50-nm organelles, which mediate the regulated exocytosis of nonpeptidergic neurotransmitters in neurons. SVs contain a well characterized set of integral membrane proteins that are involved in the various steps of their life cycle, including docking, fusion, internalization, and recycling (Calakos and Scheller, 1996). Fusion of SVs occurs at the presynaptic zone, a specialized region of the axonal membrane, and results in the release of neurotransmitter. SV membrane proteins are subsequently rapidly internalized and recycled to de novo-formed SVs (reviewed by Bauerfeind *et al.*, 1996). The classical model of SV recycling includes retrieval of membrane from the axonal membrane via clathrin-coated pits and fusion of the primary endocytic (uncoated) vesicles with endosomes (Heuser and Reese, 1973). Recycling proteins quickly enter the tubular extensions emanating from early endosome (EE) vacuoles from which they are shuttled back to the plasma membrane (Helenius *et al.*, 1983; Mayor *et al.*, 1993). SV proteins might follow a similar endosomal recycling pathway for reentering SVs. More recent evidence, however, suggests a second pathway of SV recycling, directly from the plasma membrane, without passing through an endosomal intermediate (Koenig and Ikeda, 1996; Takei *et al.*, 1996; Murthy and Stevens, 1998). SVs are retrieved directly from the plasma membrane by uncoating of the primary clathrin-coated endocytic vesicles or, after massive stimulation, from clathrin-coated tubulovesicular invaginations of the plasma membrane (Heuser and Reese, 1973; Takei *et al.*, 1996). An even faster, clathrin-independent pathway of SV formation entails reendocytosis at a transient fusion site (Fesce *et al.*, 1994). Possibly, in axons the two plasma membrane-derived pathways of SV reformation coexist with an indirect route via endosomes. The latter might be used primarily for the recycling of cell surface components and operate as a salvage recycling pathway for SV proteins (Bauerfeind *et al.*, 1996).

Neuroendocrine cells do not form axons and lack synapses and synaptic specializations but nevertheless do contain synaptic-like microvesicles (SLMVs) (Kelly, 1993a). Most information on SLMV biogenesis in neuroendocrine cells derives from the PC12 pheochromocytoma cell line.

‡ Corresponding author. E-mail address: J.Klumperman@lab.azu.nl.
Abbreviations used: AP, adaptor protein; DAB, 3,3′-diaminobenzidine tetrahydrochloride; EE, early endosome; IgG, immunoglobulin G; LE, late endosome; SLMV, synaptic-like microvesicle; Sphy, synaptophysin; SV, synaptic vesicle; TAg, T antigen tag; TfR, transferrin receptor; VAMP, vesicle-associated membrane protein.

SLMVs in PC12 cells contain the full set of SV membrane proteins identified so far (Clift-O'Grady *et al.*, 1990; Llona, 1995), have the same size as neuronal SVs (Cameron *et al.*, 1991; Linstedt and Kelly, 1991), store the neurotransmitter acetylcholine (Bauerfeind *et al.*, 1993), exclude endosomal markers such as the transferrin receptor (TfR) and low-density lipoprotein receptor (Cameron *et al.*, 1991, 1993; Linstedt and Kelly, 1991), and undergo Ca^{2+}-dependent exocytosis (Bauerfeind *et al.*, 1995). Several lines of evidence indicate the involvement of an intracellular compartment, most likely an endosomal intermediate, in the formation and reformation of SLMVs. First, synaptophysin, an integral membrane protein of SLMVs (Wiedenmann and Franke, 1985), repeatedly cycles between the plasma membrane and an internal compartment before reaching SLMVs (Régnier-Vigouroux *et al.*, 1991). Second, at steady state, the endosomes of PC12 cells contain relatively high concentrations of the SLMV membrane proteins synaptophysin and vesicle-associated membrane protein 2 (VAMP-2) (Johnston *et al.*, 1989; Cameron *et al.*, 1991; Linstedt and Kelly, 1991; Lah and Burry, 1993). Third, in transfected fibroblasts, synaptophysin is targeted to endosomes (Wiedenmann *et al.*, 1988; Johnston *et al.*, 1989; Cameron *et al.*, 1991; Linstedt and Kelly, 1991). And fourth, endocytosed HRP sequentially reaches endosomes and synaptophysin-positive SLMVs (Bauerfeind *et al.*, 1993).

The usefulness of PC12 cells as a model for SLMV recycling was furthered by the development of a cell-free system (Desnos *et al.*, 1995). In this assay, PC12 cells accumulate internalized antibodies against an epitope-tagged form of VAMP-2 at 15°C. Upon rewarming to 37°C, the internalized antibodies are delivered to SLMVs, suggesting that an intracellular intermediate functions as SLMV donor compartment. SLMV reformation from the 15°C donor compartment requires the cytosolic proteins ADP ribosylation factor-1 and adaptor protein complex AP-3 (Faúndez *et al.*, 1997, 1998), but not clathrin (Faúndez *et al.*, 1998; Shi *et al.*, 1998). In addition, Schmidt *et al.* (1997) have described a second pathway of SLMV recycling in PC12 cells, which is AP-2, dynamin, and clathrin dependent. These authors proposed the involvement of a novel compartment that is distinct from the TfR-containing endosome and connected to the plasma membrane via a narrow membrane continuity. Using different experimental conditions, the existence of a plasma membrane-derived pathway of SLMV reformation in PC12 cells was confirmed, however, only as a minor pathway (Shi *et al.*, 1998).

Morphological studies have contributed greatly to the understanding of SV formation in neurons (Heuser and Reese, 1973; Koenig and Ikeda, 1996; Takei *et al.*, 1996), because immunoelecton microscopy provides the only approach by which molecular data are directly linked to ultrastructural information. However, conclusive morphological information to extend the biochemical data obtained on the SLMV cycle in neuroendocrine cells is not yet available. Here, we have used a combination of morphological approaches to study the nature of the 15°C SLMV donor compartment and the possible involvement of endosomal intermediates in SLMV recycling in PC12 cells. Our data provide the first in situ study on SLMV formation in neuroendocrine cells and show morphological evidence for a pathway in which SLMV membrane proteins recycle from the plasma membrane to EEs before their incorporation into newly formed SLMVs.

MATERIALS AND METHODS

Cell Culture

PC12 cells (clone 251-II) were grown in Dulbecco's modified Eagle's medium supplemented with 10% horse serum and 5% fetal calf serum under 10% CO_2 at 37°C (Greene and Tischler, 1976). Under these culture conditions PC12 cells have a nonpolarized, endocrine phenotype and do not form neurites. PC12 cells stably transfected with rat T antigen-tagged VAMP-2 (VAMP-TAg) at its luminal carboxyl-terminal domain (Grote *et al.*, 1995; Grote and Kelly, 1996) were grown in Dulbecco's modified Eagle's H-21 media supplemented with 10% horse serum, 5% fetal calf serum, 100 U/ml penicillin, 100 mg/ml streptomycin, and 250 μg/ml Geneticin (G418; Life Technologies, Gaithersburg, MD) in 10% CO_2 at 37°C. Cells were treated for 18–24 h before the experiments with 6 mM sodium butyrate to increase VAMP-TAg expression.

Antibodies

We used polyclonal rabbit sera against synaptophysin (Synaptic Systems, Göttingen, Germany; McMahon *et al.*, 1996) and rab4 (Bottger *et al.*, 1996) and mouse monoclonal antibodies against clathrin (Transduction Laboratories, Lexington, KY), VAMP-2 (Cl 69.1; Edelmann *et al.*, 1995), and rab3A/B/C/D (Cl 42.1, Matteoli *et al.*, 1991). All these antibodies recognized cytosolically exposed epitopes. The latter two antibodies were kindly provided by Dr. R. Jahn (Max-Planck-Institut, Göttingen, Germany). The mouse monoclonal antibodies against the T antigen epitope TAg (KT3) and H 68.4 against the cytosolic tail of the TfR (Zymed, San Francisco, CA) have been described (White *et al.*, 1992; Desnos *et al.*, 1995). We used an affinity-purified rabbit polyclonal antiserum specific for cathepsin D (a generous gift from Dr. A. Hasilik, Philipps University, Department of Physiological Chemistry, Marburg, Germany). A bridging rabbit anti-mouse immunoglobulin G (IgG) antibody (Dako, Glostrup, Denmark) was used to provide binding sites for protein A-gold when sections were labeled with mouse monoclonal antibodies.

Internalization of BSA-gold

BSA conjugated to 5-nm colloidal gold (OD 5.0) was used as an endocytic tracer (Slot *et al.*, 1988). Before use, BSA-gold was dialyzed overnight against PBS. PC12 cells were incubated in prewarmed serum-free medium with BSA-gold for 1, 2, 3, 5, 10, or 15 min under 10% CO_2 at 37°C. For longer incubation periods, cells were pulse labeled for 15 min, quickly washed with serum-free medium, and chased for 15 or 45 min. The cells were next washed in cold culture medium and fixed for ultrathin cryosectioning as described below.

Ruthenium Red Staining

To study direct connections between intracellular compartments and the plasma membrane, PC12 cells were grown on 3.5-cm-diameter culture dishes and fixed for 60 min at 15 or 37°C with 1.2% glutaraldehyde containing 0.5 mg/ml ruthenium red (Drijfhout, Amsterdam, The Netherlands) in 66 mM cacodylate buffer, pH 7.2 (Damke *et al.*, 1994). Cells were then washed three times for 3 min with 150 mM cacodylate buffer, pH 7.2, and postfixed for 3 h at room temperature with 1.3% OsO_4 and 0.5 mg/ml ruthenium red in 33 mM cacodylate buffer, pH 7.2. Finally, the cells were washed three times for 5 min with 150 mM cacodylate buffer, pH 7.2, and processed for embedding in Epon. Ultrathin sections were stained with lead citrate and uranyl acetate.

Table 1. Progression of endocytosed BSA-gold through the endosomal pathway in PC12 cells

time of BSA-gold uptake (min) at 37°C	primary endocytic vesicles	EEs	LEs	lysosomes
1	68 ± 7.0	30 ± 6.2	2 ± 3.8	0
2	47 ± 7.6	40 ± 2.3	13 ± 6.5	0
3	29 ± 5.8	53 ± 3.4	18 ± 5.2	0
5	19 ± 2.6	52 ± 0.9	29 ± 4.0	0
10	8 ± 0.6	24 ± 0.9	68 ± 1.0	0
15	8 ± 0.5	21 ± 0.5	71 ± 2.5	0
15+15	2 ± 0.3	4 ± 0.5	83 ± 2.6	1 ± 0.5
15+45	1 ± 0.2	1 ± 0.2	46 ± 1.3	52 ± 0.5

BSA-gold was taken up for 1–15 min continuously or for 15 min of pulse and 15 or 45 min of chase. The numbers are mean percentages of total gold particles ± SD found in four morphologically distinct types of endocytic compartments.

Immunoelectron Microscopy of Ultrathin Cryosections

Cells were prepared for ultrathin cryosectioning and double immunogold labeled according to the protein A-gold method as previously described (Geuze *et al.*, 1981; Slot *et al.*, 1988, 1991). Briefly, cells were fixed in 2% formaldehyde and 0.2% glutaraldehyde in 0.1 M phosphate buffer for 2 h at room temperature, stored overnight at 4°C in 2% formaldehyde and 0.2% glutaraldehyde in 0.1 M phosphate buffer, and washed in PBS with 0.02 M glycine. Fixed cells were scraped off the dish and embedded in 10% gelatin in PBS, which was solidified on ice and cut into small blocks. After infiltration with 2.3 M sucrose at 4°C, blocks were mounted on aluminum pins and frozen in liquid nitrogen. Ultrathin cryosections were picked up in a mixture of 50% sucrose and 50% methyl cellulose, which results in improved preservation of ultrastructure (Liou *et al.*, 1996).

Morphometrical Analysis

Semiquantitative analysis of the distribution patterns of internalized 5 nm BSA-gold and SLMV proteins was carried out as follows. Areas on cryosections with good ultrastructure were selected at low magnification and scanned at 20,000× along a fixed track. All gold particles within a distance of 30 nm from membranes were counted as positive and assigned to the compartment over which they were located. For each quantitative analysis, at least four independent quantitations were performed. The distribution of gold particles was expressed as percentage of total gold particles found over a specific intracellular compartment. To establish the relative distribution of internalized BSA-gold uptake (Table 1), 500 gold particles were counted after 1 and 2 min of uptake, 1000 after 3 min, 5000 after 5 min, and 7500 after 30 and 60 min uptake. To establish the relative distribution patterns of synaptophysin and VAMP-2 in endocytic compartments of PC12 cells (Table 2), 4000 and 2500 gold particles were counted, respectively. To establish the colocalization between rab3 and synaptophysin in double-labeled sections, 145 randomly encountered rab3-positive SLMVs were analyzed for the presence of synaptophysin. The relative intracellular distribution of VAMP-TAg (see Table 4) was established by counting 500 gold particles at 15°C, and 1000 and 1500 gold particles after 5 and 25 min of warming to 37°C, respectively. In a separate counting, the relative distribution of VAMP-TAg over the vacuolar part of EEs and the tubules emanating from the vacuole was established. For this purpose, 70 EEs of cells that had taken up VAMP-TAg for 40 min at 15°C and 70 EEs of cells that after 40 min at 15°C were subsequently rewarmed for 5 min to 37°C were analyzed. In our quantitative studies, only those tubules and vesicles that were visibly connected to or at a maximum distance of 100 nm from an endosomal vacuole, were considered as endosome-associated tubules or vesicles.

Uptake of the KT3 Antibody

To study the internalization pathway of VAMP-2, PC12 cells expressing VAMP-TAg/N49A were used. The point mutation in the cytoplasmic tail was previously shown to enhance VAMP-2 targeting to SLMVs (Grote and Kelly, 1996), and the epitope tag (TAg) on the luminal domain allows labeling of cells in culture with the KT3 antibody. VAMP-TAg cells grown to 70% confluency in 6-cm-diameter culture dishes were kept for 1 h at 37°C in serum-free culture medium, followed by a wash in cold uptake buffer (PBS with 3% BSA, 0.3 mM $CaCl_2$, 0.3 mM $MgCl_2$, and 1 mg/ml glucose). KT3 antibodies were allowed to bind for 15 min on ice, followed by a 40-min incubation at 15°C (Lichtenstein *et al.*, 1998). Subsequently, cells were fixed, or antibodies bound to the plasma membrane were removed by washing with uptake buffer, after which cells were warmed to 37°C for 0, 5, or 25 min. Finally, the cells were washed four times with ice-cold uptake buffer, fixed in 2% formaldehyde and 0.2% glutaraldehyde, and processed for cryosectioning. Visualization of internalized KT3 antibodies by labeling with a rabbit anti-mouse IgG antibody and protein A-gold resulted in the labeling of ~15–20% of the cells, consistent with a differential expression level of VAMP-TAg between cells.

Whole-Mount Immunoelectron Microscopy of Isolated SLMV Donor Compartments

VAMP-TAg/N49A PC12 cells grown on 15-cm culture dishes were incubated for 1 h at 37°C in serum-free media and washed in ice-cold uptake buffer. The cells were next preincubated for 15 min on ice with 10 mg/ml HRP in uptake buffer, followed by an incubation for 40 min at 15°C. The cells were subsequently washed four times for 2 min each with ice-cold uptake buffer and homogenized as described (Clift-O'Grady *et al.*, 1998), and an endosomal fraction was generated by spinning the homogenates for 5 min at 1000 × *g* and subjecting supernatants to an additional spin of 5 min at 10,000 × *g* to generate 50-kg/min supernatants (Lichtenstein *et al.*, 1998). Endosomes were pelleted from 50-kg/min supernatants by centrifugation for 35 min at 27,000 × *g*, resuspended in 1.5% glutaraldehyde in 0.1 M cacodylate buffer, and incubated for 10 min on ice. To quantitatively pellet membranes for electron microscopic analysis, the fixed fraction was centrifugated for 30 min at 100,000 × *g*, after which the pellet was washed in 0.1 M cacodylate buffer, pH 6.9. Then the pellet was preincubated for 15 min with 10 mg/ml 3,3′-diaminobenzidine tetrahydrochloride (DAB) in 0.1 M cacodylate buffer, pH 6.9, and incubated for additional 45 min at room temperature in the presence of 0.01% H_2O_2 (in the dark). The DAB stained pellet was washed two times with 0.1 M cacodylate buffer, pH 6.9, and resuspended in 0.1 M phosphate buffer, pH 7.4. Five microliters of the suspension were put on a Formvar-carbon–coated copper grid, air dried for 30 min at room temperature, and washed five times for 3 min each with distilled water and 5 min with PBS. SLMV membrane proteins on these whole-mount fractions were visualized by immunogold labeling of the grids as described (Glickman *et al.*, 1996). Finally, the grids were embedded in a layer of 2% methylcellulose and uranyl acetate, pH 4.

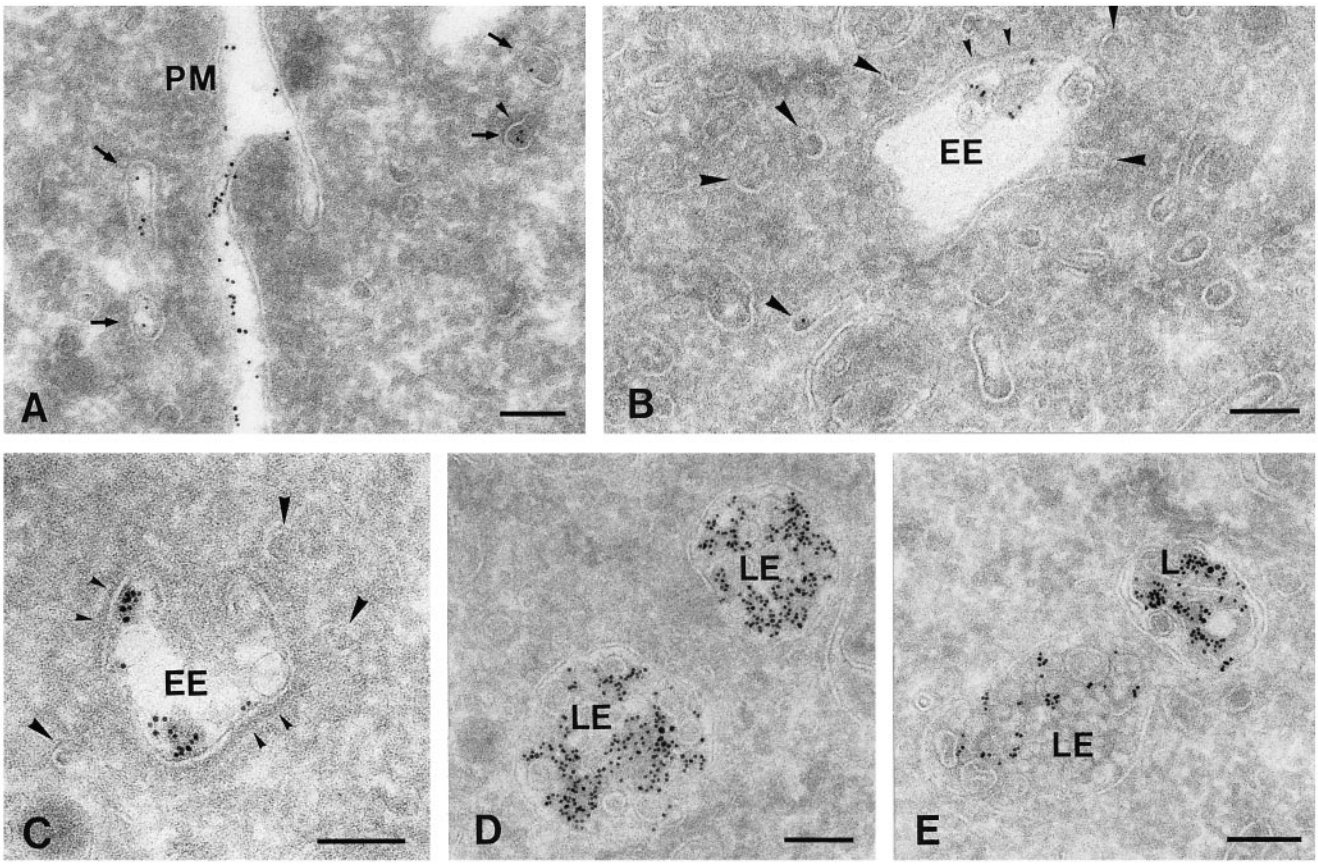

Figure 1. Overview of the distinct endosomal intermediates in PC12 cells as observed in ultrathin cryosections. Cells were allowed to internalize 5-nm BSA-gold for different periods at 37°C (A, 2 min; B and C, 15 min; D, 15 min pulse and 15 min chase; E, 15 min pulse and 45 min chase). Four morphologically distinct types of endocytic compartments could be distinguished (also see Table 1). (A) Primary ~85-nm endocytic vesicles and tubules (arrows) in the vicinity of the plasma membrane (PM). Some primary endocytic vesicles were decorated with a clathrin coat (small arrowhead). (B and C) EEs were characterized by their elongated, sometimes curved (C), vacuolar part with few internal vesicles. Large domains of the limiting membrane of EEs displayed a clathrin coat (small arrowheads; also see Figure 3E). Associated or connected with the vacuolar domain of EEs were numerous ~40-nm tubules and vesicles (large arrowheads). (D and E) LEs exhibited a more regular, rounded shape and many internal vesicles. Lysosomes (L) became labeled between 30 and 60 min of internalization and had an electron-dense content, a variable shape, and sometimes internal membrane sheets. Bars, 100 nm.

RESULTS

Characterization of the Endosomal Pathway in PC12 Cells

To investigate a possible role of endocytic compartments in SLMV protein endocytosis and recycling, we first set out to define the endocytic compartments of PC12 cells at the ultrastructural level by a number of morphological methods. First, we performed a quantitative analysis of the progression of endocytosed tracer (BSA-gold) through endosomal subcompartments. We found four morphologically distinct types of endocytic compartments, which were sequentially reached by BSA-gold (Table 1). After 1 min of internalization, the majority (~70%) of tracer was found in ~80- to 90-nm primary endocytic vesicles and tubules, some of which displayed the electron-dense cytosolic coating characteristic of clathrin (Figure 1A). Approximately 30% of the BSA-gold was found in sorting EEs, which consisted of an elongated, sometimes curved electron lucent vacuole with few internal vesicles (Figure 1, B and C). These internal vesicles arise by microautophagy from the EE vacuolar membrane, and their number increases upon maturation of the endosomes (reviewed by Geuze, 1998). Large domains of the limiting membrane of these vacuolar EEs were decorated with clathrin (Figure 1, B and C; see Figure 3E), sometimes evolving into clathrin-coated buds, as has previously been described for EEs in hepatocytes (Geuze *et al*., 1984) and fibroblasts (Stoorvogel *et al*., 1996). Connected to or in close association with the EE vacuoles, many ~35- to 45-nm tubulovesicular profiles were present (Figure 1, B and C), which were devoid of BSA-gold at short incubation times. These tubulovesicular profiles were previously identified as the tubular extensions of EEs involved in protein recycling (Geuze *et al*., 1984; Klumperman *et al*., 1993; Marsh *et al*., 1986; Slot *et al*., 1991). In PC12 cells, recycling tubules and vesicles could clearly be distinguished from primary endocytic vesicles by their smaller size and often ellipsoid shape (Figure 1, compare A with B and C). Measurements of 25

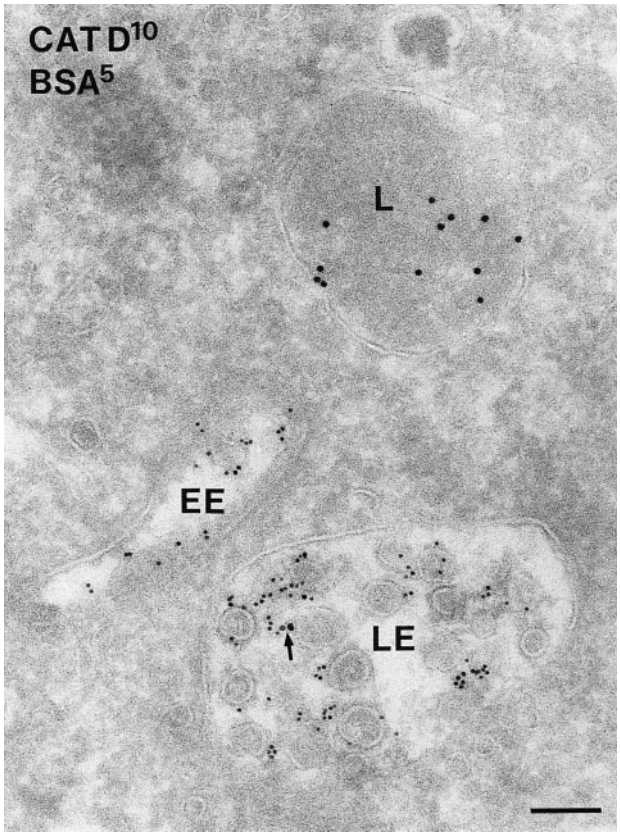

Figure 2. Immunogold labeling for the lysosomal enzyme cathepsin D (10-nm gold) is predominantly present in an electrondense lysosome (L). The arrow points to low labeling in an LE. Five-nanometer BSA-gold was internalized for 15 min and is present in both an EE and a LE but absent from the lysosome. Bar, 100 nm.

recycling vesicles revealed a mean diameter of 41.3 ± 4.1 nm (average ± SD), whereas in a similar measurement for endocytic vesicles this amounted to 86.1 ± 11.2 nm.

Late endosomes (LEs) differed from EEs by their more globular shape, numerous internal vesicles, and a less frequent clathrin coat (Figures 1, D and E, and 2). Although the front of endocytosed BSA-gold reached these endosomes after relatively short periods, the bulk was detected after 10 min of uptake (Table 1). Electron-dense lysosomes (Figures 1E and 2) started to fill with BSA-gold after 30 min of internalization. The lysosomal enzyme cathepsin D was by immunogold staining absent from EEs, whereas low amounts were found in LEs, and lysosomes were densely labeled (Figure 2).

Schmidt *et al.* (1997), have proposed narrow-necked invaginations of the plasma membrane as the major donor compartment for SLMVs in PC12 cells. In thin sections, narrow connections are not always detectable. Therefore, to unequivocally distinguish between free and plasma membrane-attached compartments, cells were fixed in the presence of ruthenium red at 15 and 37°C to stain the plasma membrane and its invaginations. As is shown in Figure 3, B and C, EEs were negative for ruthenium red. Sometimes we observed clathrin-coated vesicles that, although seemingly intracellular, were stained for ruthenium red (Figure 3A), indicating that they were in fact deep invaginations of the plasma membrane and reinforcing the notion that apparently free structures can still be attached to the plasma membrane (Schmid and Smythe, 1991; Damke *et al.*, 1994). Similar data were obtained in cells fixed at 37°C (our unpublished results). Importantly, this approach demonstrated that EEs are free compartments and not invaginations of the plasma membrane.

In an alternative approach to distinguish EEs from plasma membrane invaginations, sections were immunogold labeled for the small GTPase rab4, an EE marker that is absent from the plasma membrane (van der Sluijs *et al.*, 1991, 1992; Bottger *et al.*, 1996; Daro *et al.*, 1996; Ayad *et al.*, 1997). As shown in Figure 3D, rab4 labeling in PC12 cells was found over EEs and associated vesicles but not at the plasma membrane, confirming that what we refer to as EEs are compartments distinct from the plasma membrane.

EEs Contain High Levels of SLMV Proteins

We next studied the steady state distribution of the SLMV proteins synaptophysin (Navone *et al.*, 1986; Wiedenmann *et al.*, 1988) and VAMP-2 (Trimble *et al.*, 1988). Both proteins exhibited a similar labeling pattern, although the labeling density of VAMP-2 was consistently less than that of synaptophysin. At steady state, only ~5% of total gold particles of both proteins were found over the Golgi stack, consistent with the long half-life (in the order of days) of SLMV membrane proteins (reviewed by Calakos and Scheller, 1996). Importantly, approximately one-third of total labeling of both SLMV proteins was confined to endocytic compartments, especially to the EE-associated tubules and vesicles (Figure 4, A and B, and Table 2). LEs and lysosomes contained little if any of the SLMV marker proteins (Table 2), suggesting that the EEs are the only endocytic intermediates with a putative role in SLMV formation.

Characterization of SLMVs in PC12 Cells

The majority (>60%) of synaptophysin and VAMP-2 gold label was present on noncoated ~40-nm vesicles and tubules. These vesicles were found in close proximity to EEs (Figure 4) and the *trans*-Golgi area (Figure 5B) and in the cell periphery, occasionally clustered in groups (e.g., Figures 5A and 6, E and F). Double immunogold labeling showed that endogenous synaptophysin and VAMP-2 (Figure 6C) as well as internalized VAMP-TAg (Figure 6F; also see below) colocalized to a high extent in these vesicles. To discriminate these putative SLMVs from constitutive recycling vesicles, we performed a double labeling of synaptophysin and the TfR. TfR recycling to the plasma membrane is mediated by constitutive recycling vesicles, and TfR is absent from SLMVs (Cameron *et al.*, 1991; Linstedt and Kelly, 1991). TfR was found on primary endocytic vesicles (Figure 6A), EEs, where it predominated on the associated vesicles and tubules (Figure 6B), and vesicles that were morphologically similar to the vesicles containing high levels of synaptophysin and VAMP-2 (Figure 5). Most of these TfR-positive vesicles were found in the Golgi area (Figure 5B), whereas small vesicles near the plasma membrane mostly lacked TfR and were almost exclusively labeled for synaptophysin (Figure 5A). Of all synaptophysin-positive small vesi-

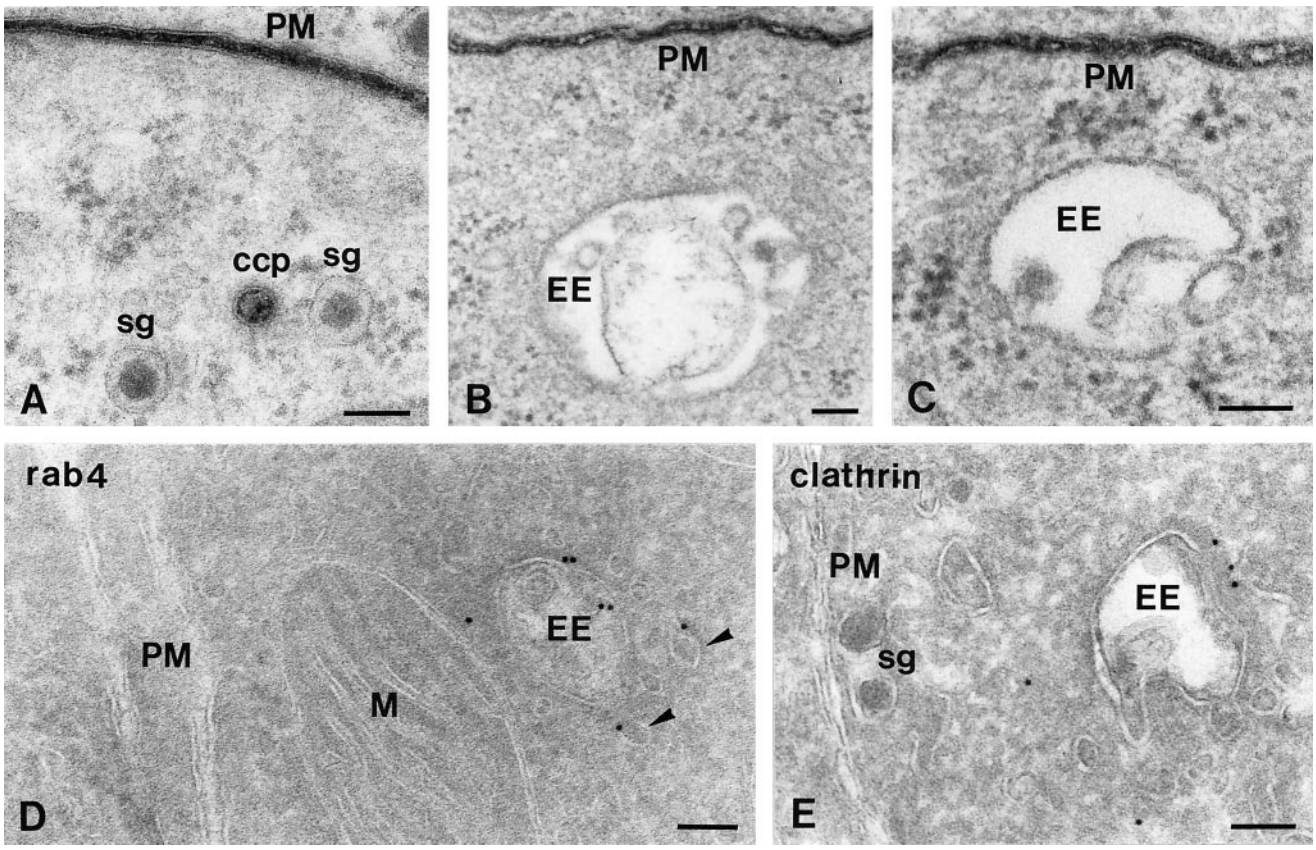

Figure 3. EEs are not connected to the plasma membrane (PM). (A–C) Ultrathin Epon sections of PC12 cells fixed at 15°C in the presence of the membrane-impermeable reagent ruthenium red (electron-dense staining) to mark all plasma membrane-associated structures. (D and E) Ultrathin cryosections of PC12 cells immunogold labeled for rab4 (D) or clathrin (E). (A) Ruthenium red staining was clearly visible at the PM and constricted clathrin-coated pits (CCP). (B and C) By contrast, EEs were consistently negative for ruthenium red. (D) The small GTPase rab4 (10-nm gold) is found on EE vacuoles and associated tubules and vesicles (arrowheads) but absent from the PM. (E) The electron-dense coating of EE vacuole contains clathrin (10-nm gold). M, mitochondrion; sg, secretory granule. Bars, 100 nm.

cles, only a minor fraction contained TfR (Figure 5). A further characterization of the synaptophysin-positive SLMVs was carried out by immunolocalization of rab3, a small GTPase that transiently associates with SVs (Matteoli *et al.*, 1991), but not with vesicles involved in constitutive recycling (Bean and Scheller, 1997). Figure 6, D and E, shows that rab3 and synaptophysin colocalize to vesicles in close vicinity to EEs and similar vesicles adjacent to the plasma membrane. Quantitative analysis of this colocalization revealed that 78% of the rab3-positive vesicles also labeled for synaptophysin. Taken together, both the size and molecular makeup of the majority of the SLMVs in PC12 cells meet the characteristics of neuronal SVs.

SLMV Proteins Are Separated from the TfR in EEs

The high densities of synaptophysin and VAMP-2 in EE tubules and in SLMVs associated with EEs suggested a role for EEs in SLMV formation. If SLMVs arise from EEs, this would imply sorting of SLMV proteins from the TfR at the exit of EEs, because both types of proteins are present in EE vacuoles, whereas the TfR is absent from SLMVs. To study this putative sorting event, we established the degree of colocalization of the TfR and the SLMV markers VAMP-2 and synaptophysin in primary endocytic vesicles (which deliver the two proteins to EEs), and in EE tubules (the exit sites of EEs). To distinguish between these two categories we used strict definitions. Based on the BSA-gold uptake experiments (Figure 1 and Table 1) and our size measurements, primary endocytic vesicles were defined as ~85-nm, sometimes coated vesicles and tubules, close to the plasma membrane (e.g., Figures 1A, 3A, and 5A). EE tubules were defined as ~40-nm tubulovesicular profiles that were connected to or closely associated with the vacuolar part of EEs (e.g., Figures 1, B and C, 4, A and B, and 6, B–D). Although EE tubules extended to a considerable distance from EEs, for this quantitation we only considered EE tubules and vesicles that were within 100 nm from an EE vacuole. We found that synaptophysin and TfR codistributed in 36 ± 3% of the primary endocytic vesicles, whereas they hardly shared EE tubules and vesicles as a common site (Table 3). In contrast, synaptophysin and VAMP-2 colocalized in 45 ± 4% of the primary endocytic vesicles and in 38 ± 3% of the EE tubules and vesicles. Thus, although TfR and the SLMV marker synaptophysin exhibited a high degree of colocalization in incom-

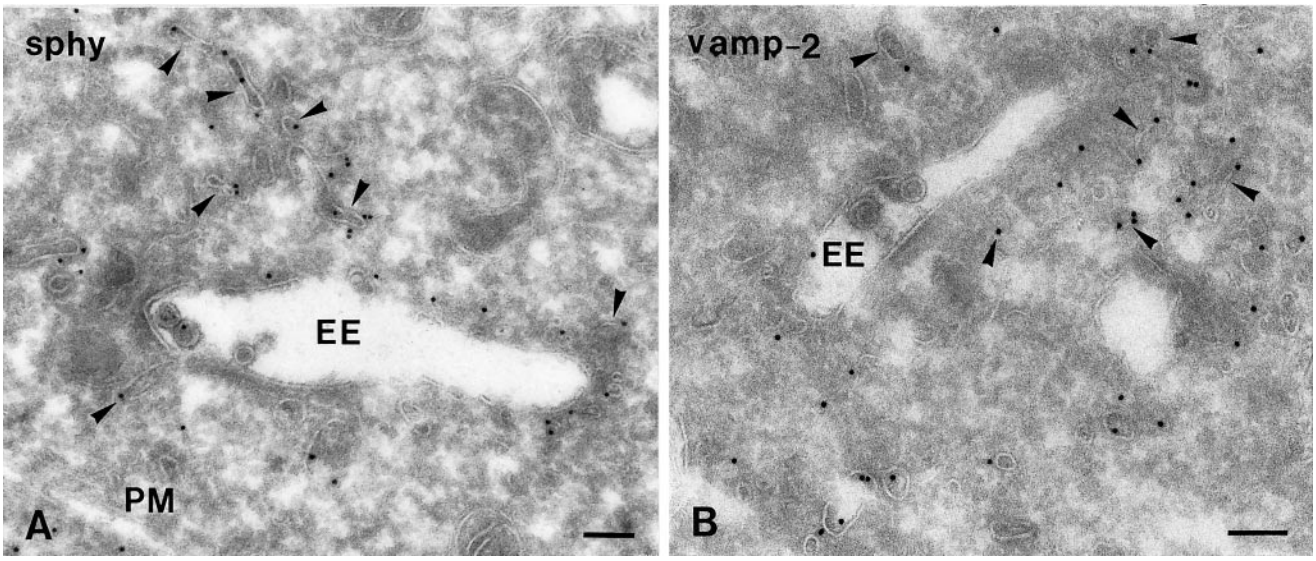

Figure 4. Ultrathin cryosections of PC12 cells showing 10-nm immunogold labeling of synaptophysin (A, sphy) and VAMP-2 (B). Both SLMV marker proteins are predominantly present in EE-associated tubules and vesicles (arrowheads). PM, plasma membrane. Bars, 100 nm.

ing endocytic vesicles, after transit of the EEs they were largely separated.

Internalization and Recycling of Epitope-tagged VAMP-2 through EEs

To further investigate the possibility that SLMV proteins recycle through EEs, we investigated VAMP-2 transport in the VAMP-TAg/N49A PC12 transfectant. Using cell fractionation, it was previously shown that VAMP-TAg/PC12 cells internalize the KT3 monoclonal antibody and recycle the KT3/VAMP-TAg complex to SLMVs (Grote *et al.*, 1995). At 15°C, the internalized VAMP-TAg accumulates in an SLMV donor compartment, from which SLMVs are reformed upon warming to 37°C (Desnos *et al.*, 1995).

Here we applied this temperature shift protocol in a morphological approach. VAMP-TAg/PC12 cells were allowed to internalize the KT3 antibody for 40 min at 15°C. The internalized antibodies were visualized by immunogold labeling of ultrathin cryosections with a rabbit anti-mouse IgG antibody. Endocytosis of VAMP-TAg occurred via clathrin-coated vesicles that were indistinguishable from the vesicles involved in BSA-gold uptake (Figure 7*A*). For a semiquantitative analysis of the recycling pathway of KT3, plasma membrane-associated antibody was washed away, and the cells were rewarmed to 37°C for 0, 5, or 25 min before fixation (Figure 7, B–E, and Table 4). Table 4 shows the subcellular distribution of internalized VAMP-TAg at the various conditions. Importantly, at 15°C, internalized VAMP-TAg was found in EE sorting vacuoles, but EE tubules were largely devoid of VAMP-TAg (Figure 7, B and C). Upon rewarming, there was a rapid depletion of VAMP-TAg from primary endocytic vesicles and a shift toward EE tubules and vesicles and SLMVs (Figure 7, D and E, and Table 4). VAMP-TAg-positive SLMVs were found near EEs, in the Golgi area, and underneath the plasma membrane, resembling the distribution of SLMVs visualized by labeling for endogenous VAMP-2 and synaptophysin. Accordingly, VAMP-TAg and synaptophysin showed a high level of colocalization in SLMVs (Figure 6F).

A small portion (~8%) of VAMP-TAg appeared in LEs and lysosomes, showing the partial targeting of VAMP-TAg to the degradative pathway (Table 4). However, consistent with previous in vitro studies (Desnos *et al.*, 1995), a signif-

Table 2. Relative distributions of synaptophysin and VAMP-2 over distinct endocytic subcompartments in PC12 cells

	Primary endocytic vesicles	EEs		LEs	Lysosomes
		Vacuole	Tubules/vesicles		
Synaptophysin	24 ± 1.4	24 ± 2.1	46 ± 3.0	5 ± 1.5	1 ± 0.6
VAMP-2	36 ± 2.8	12 ± 2.8	43 ± 3.5	7 ± 2.4	2 ± 1.0

The numbers represent the mean percentages of total gold particles ± SD found over the indicated compartments. EEs were divided into a vacuolar subdomain and ~40-nm associated tubules and vesicles.

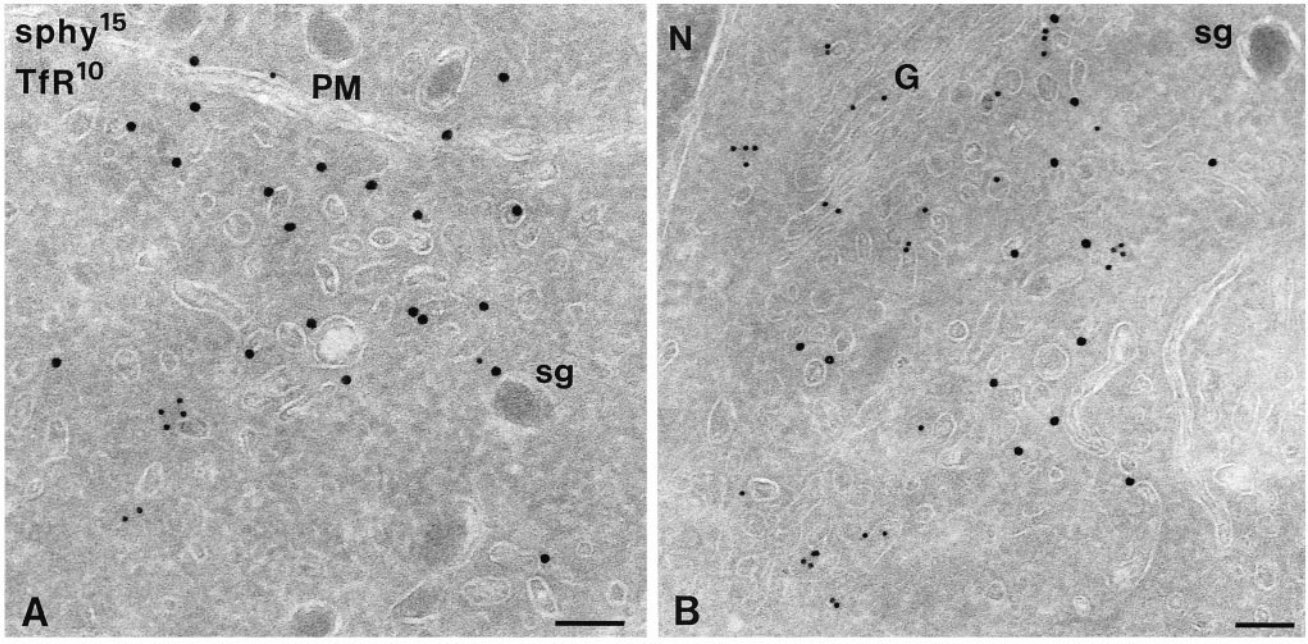

Figure 5. PC12 cells double immunogold labeled for synaptophysin (sphy, 15-nm gold) and TfR (10-nm gold). (A) Close to the plasma membrane (PM), clusters of small vesicles are present that contain sphy but not TfR. (B) In the Golgi (G) area, sphy-positive as well as TfR-positive vesicles are found. N, nucleus; sg, secretory granule. Bars, 100 nm.

icant amount of internalized VAMP-TAg was correctly delivered to SLMVs.

Table 4 shows an important redistribution of internalized VAMP-TAg in EEs from the vacuolar toward the tubular subdomains after rewarming. This suggests that VAMP-TAg exits the EE through the associated tubules. To investigate this in more detail, we studied in a separate quantitative analysis the relative distribution of VAMP-TAg between the vacuolar and tubulovesicular parts of EEs in 70 randomly encountered EEs, at both 15 and 37°C. Again, only connected vesicular-tubular profiles and those within 100 nm from the EE vacuole were taken into account. After 40 min of internalization at 15°C, ~90% of VAMP-TAg was found in the vacuolar part of EEs, and only ~10% was found in the associated tubulovesicular profiles. After a subsequent 5-min incubation at 37°C, the vacuolar labeling of VAMP-TAg decreased to 63%, whereas the labeling in EE tubulovesicular profiles increased to 37%. These data identify EE sorting vacuoles as the compartment where internalized VAMP-TAg accumulates at 15°C (Desnos *et al*., 1995) and show that only after rewarming to 37°C, VAMP-TAg enters the tubular extensions that emanate from EE vacuoles. In ultrathin cryosections cross-sections through tubules cannot always be distinguished from free vesicles. Vesicular profiles near EEs therefore likely included both EE tubules and SLMVs. Importantly, however, our data show that rewarming to 37°C is required for the occurrence of endocytosed VAMP-TAg in both EE tubules and SLMVs. These data strongly suggest that internalized VAMP-TAg recycles through the vacuolar part of EEs to the associated tubules, and that SLMVs are formed by budding from EE tubules. After prolonged incubation at 37°C, labeling of SLMVs increased at the expense of EEs (Table 4), which is consistent with this interpretation.

Isolated SLMV Donor Compartments Are Identical to EEs

In a previous study we described a cell fractionation procedure to enrich for an SLMV donor compartment in which internalized VAMP-TAg accumulates at 15°C (Lichtenstein *et al*., 1998). Our present in vivo data suggest that this accumulation occurs in the EE vacuole. To investigate the relation between the 15°C SLMV donor compartment and the EEs as defined by our morphological assays, we analyzed isolated SLMV donor compartments by whole-mount immunoelectron microscopy. In short, VAMP-TAg/PC12 cells were allowed to internalize HRP for 40 min at 15°C. The cells were subsequently homogenized and centrifugated to generate a 50-kg/min supernatant that contains much of the SLMV donor activity (Lichtenstein *et al*., 1998). Whole-mount electron microscopy analysis of this fraction showed 300- to 400-nm structures, with a morphology compatible with EEs in situ (Figure 8, compare A with B and C). The isolated SLMV donor compartments contained DAB polymer indicative for the presence of internalized HRP and confirming their endocytic nature. Finally, immunogold labeling showed the presence of both synaptophysin (Figure 8C) and VAMP-2 (our unpublished results) on the isolated SLMV precursor compartments. Together these data are compatible with the 15°C SLMV in vitro donor compartment being the EE vacuole.

DISCUSSION

Our data indicate that the tubular extensions of EEs can function as donor compartments for newly formed SLMVs

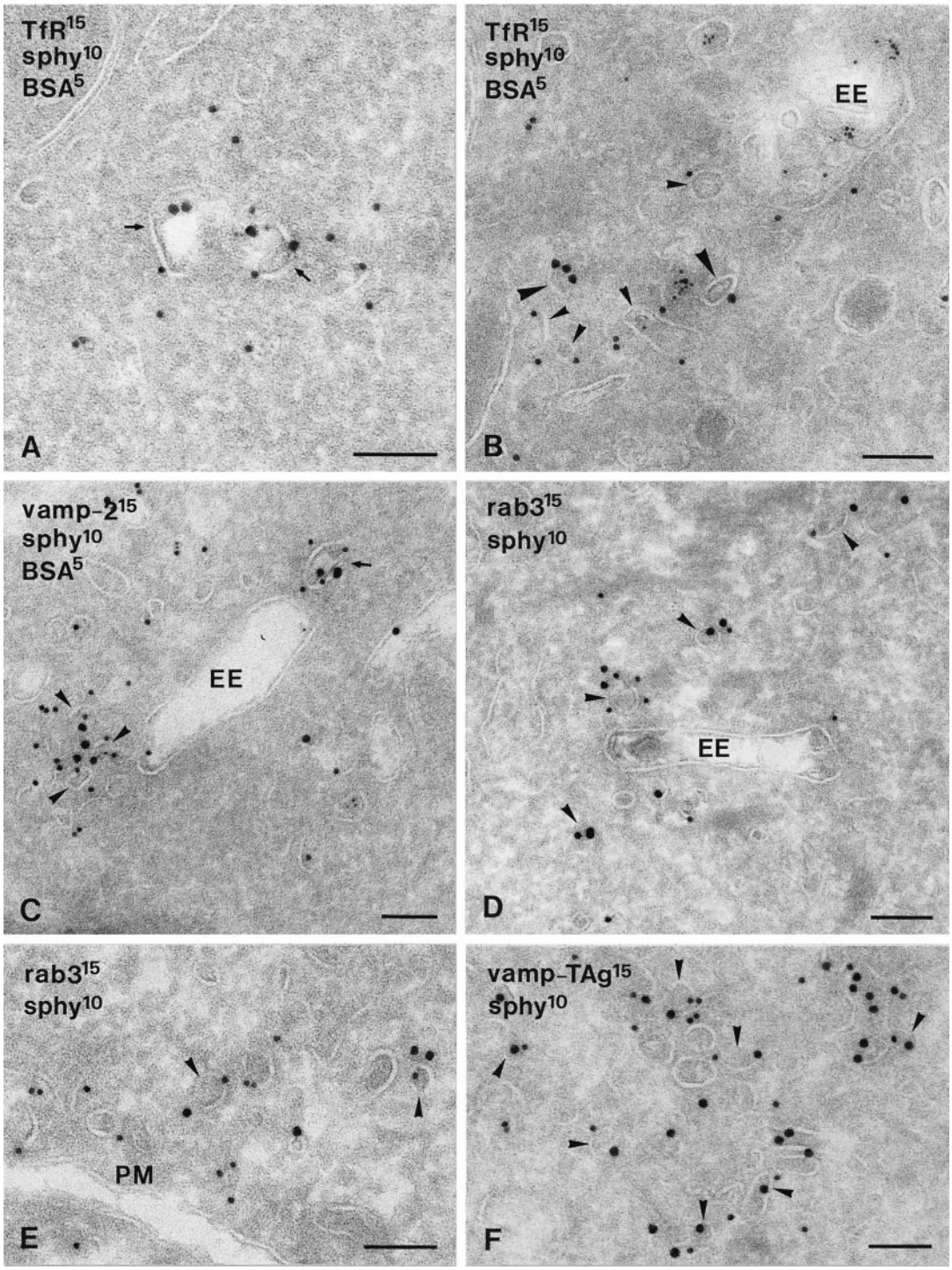

Figure 6. Ultrathin cryosections of PC12 cells. Cells were incubated with 5-nm BSA-gold for 40 min at 15°C to mark early endocytic compartments and rewarmed to 37°C for 5 min to accumulate proteins at the EE exits (A–C). (A and B) Double immunogold labeling for TfR (15-nm gold) and synaptophysin (sphy, 10-nm gold). TfR and synaptophysin localized to the same primary endocytic vesicle (A, arrows), whereas most EE-associated tubules and vesicles contained either TfR (B, large arrowheads) or synaptophysin (B, small arrowheads). (C) VAMP-2 (15-nm gold) and synaptophysin (10-nm gold) colocalized to a high extent in both primary endocytic vesicles (arrow) and EE-associated tubules and vesicles (arrowheads). (D and E) Rab3 (15-nm gold) and synaptophysin (10-nm gold) colocalized to SLMVs in close proximity to EEs (D, arrowheads) and the plasma membrane (PM; E, arrowheads). (F) VAMP-TAg/KT3 (15-nm gold), internalized for 40 min at 15°C and 5 min at 37°C (for details, see the legend of Figure 7), and endogenous synaptophysin (10-nm gold) colocalized in clusters of vesicles (arrowheads), similar in appearance to the rab3-positive SLMVs in E. Bars, 100 nm.

Table 3. Colocalization of TfR and VAMP-2 with synaptophysin in EE import and export intermediates

	Primary endocytic vesicles				EE-associated tubules/vesicles			
Synaptophysin	+	+	−		+	+	−	
TfR	+	−	+	n	+	−	+	n
	36 ± 3	39 ± 4	24 ± 3	289	6 ± 2	63 ± 3	31 ± 3	378
Synaptophysin	+	+	−		+	+	−	
VAMP-2	+	−	+	n	+	−	+	n
	45 ± 4	38 ± 2	17 ± 2	305	38 ± 3	41 ± 5	21 ± 3	433

Primary endocytic vesicles and EE-associated tubules and vesicles were characterized for their content in double immunogold-labeled sections. Primary endocytic vesicles were defined as ~85-nm sized and close to the plasma membrane. EE-associated tubules and vesicles were ~40-nm sized and connected with or at a distance of ≤100 nm from the vacuolar part of EEs. Numbers represent the percentages of total vesicles that contained the indicated proteins and are the means of three counting sessions ± SD.

in nondifferentiated PC12 cells. First, we identified EEs as heterogeneously sized and shaped, clathrin-coated, rab4-positive compartments that were reached by internalized BSA-gold after 1 min of uptake and did not stain for the plasma membrane marker ruthenium red. Second, we showed that at steady state high levels of SLMV proteins were found in tubules emanating from EEs and in rab3-positive SLMVs in close vicinity to EEs. Third, we found that at 15°C, a condition in which internalized SLMV proteins do not enter SLMVs, internalized VAMP-TAg accumulated in EE vacuoles and did not enter the EE tubules. Only after rewarming to 37°C did VAMP-TAg enter endosomal tubules and simultaneously appear in numerous newly formed SLMVs. Finally, morphological analysis of isolated SLMV donor compartments revealed the presence of EE-like compartments.

Our morphological characterization of the endocytic pathway in PC12 cells (Figure 1 and Table 1) revealed that the endocytic compartments in this cell line are very similar to those of nonneuroendocrine cells (Griffiths *et al.*, 1989; Klumperman *et al.*, 1993; Kleijmeer *et al.*, 1997). Neither the morphology of the distinct endocytic intermediates nor the distribution patterns of synaptophysin, VAMP-2, and the TfR provided any clues for the existence of a specialized endosome dedicated to SLMV recycling (Kelly, 1993b). In agreement with earlier studies (Cameron *et al.*, 1991; Linstedt and Kelly, 1991; Lah and Burry, 1993; Grote *et al.*, 1995; Grote and Kelly, 1996), synaptophysin and VAMP-2 were mainly found on EEs as opposed to LEs and lysosomes, especially on the EE tubules and vesicles, which identified these organelles as the most likely candidates for the intracellular SLMV donor compartment.

A prerequisite to analyze SLMV trafficking at the ultrastructural level was a reliable morphological definition of SLMVs in PC12 cells. Such a characterization was hampered by the fact that SLMVs do not cluster in specialized presynaptic areas, as in neurons. Furthermore, established SLMV marker proteins such as synaptophysin also localize to constitutive recycling vesicles (Régnier-Vigouroux *et al.*, 1991). To establish the relative occurrence of SLMV proteins in constitutive recycling vesicles, cells were double labeled for TfR and synaptophysin. Within the *trans*-Golgi area, approximately equal levels of labeling were found for these two proteins (Figure 5), but at some distance from the Golgi the huge majority of small vesicles were positive for synaptophysin and negative for the TfR. SLMVs were further identified by the presence of the small GTPase rab3, which is known to selectively associate with SVs and secretory granules but not with vesicles involved in constitutive recycling (Bean and Scheller, 1997). Double immunogold labeling for synaptophysin and rab3 showed the association of rab3 with synaptophysin-positive vesicles. Rab3-positive SLMVs were found close to EEs, in the Golgi area, and underneath the plasma membrane. Despite the fact that SLMVs are not docked in specialized areas of the cells, we regularly observed small clusters of SLMVs, which could be stained for rab3, synaptophysin, and VAMP2 and were negative for TfR. Also, internalized VAMP-TAg appeared in clusters of SLMVs upon rewarming to 37°C, where it colocalized to a high extent with synaptophysin (Figure 6F). Together these data indicate that the huge majority SLMV protein-positive ~40-nm vesicles were SLMVs and not constitutive recycling vesicles.

If SLMV biogenesis were to occur from EEs, it should be preceded by an endosomal sorting event, because TfR is present on EEs but absent from SLMVs. By quantifying the degree of codistribution of TfR and the SLMV marker synaptophysin, we observed an 83% decrease in colocalization between the EE import and export intermediates (Table 3). With this observation we pinpointed this endosomal sorting event at the level of recycling vesicles and tubules emanating from EE vacuoles. To more directly assay the SLMV protein recycling pathway, we next studied the internalization kinetics of epitope-tagged VAMP-2 by quantitative immunoelectron microscopy. VAMP-TAg was taken up via clathrin-coated vesicles and delivered to EEs. At 15°C, internalized VAMP-TAg accumulated in the vacuolar part of EEs. Subcellular fractionation has shown that under this condition internalized VAMP-TAg accumulates in an intracellular compartment from which SLMVs can be formed upon warming to 37°C (Desnos *et al.*, 1995; Lichtenstein *et al.*, 1998). Indeed, after release of the 15°C block, VAMP-TAg appeared within 5 min in SLMVs. Notably, this redistribution was accompanied by a significant shift of intraendosomal VAMP-TAg from the vacuolar portion of EEs to the associated tubular extensions. The observation that SLMV proteins enter EE tubules before SLMVs start to reform suggests that SLMVs form from the tubular extensions of EEs and not the EE vacuole. Together the data indicate that internalized VAMP-TAg recycles through the vacuolar part

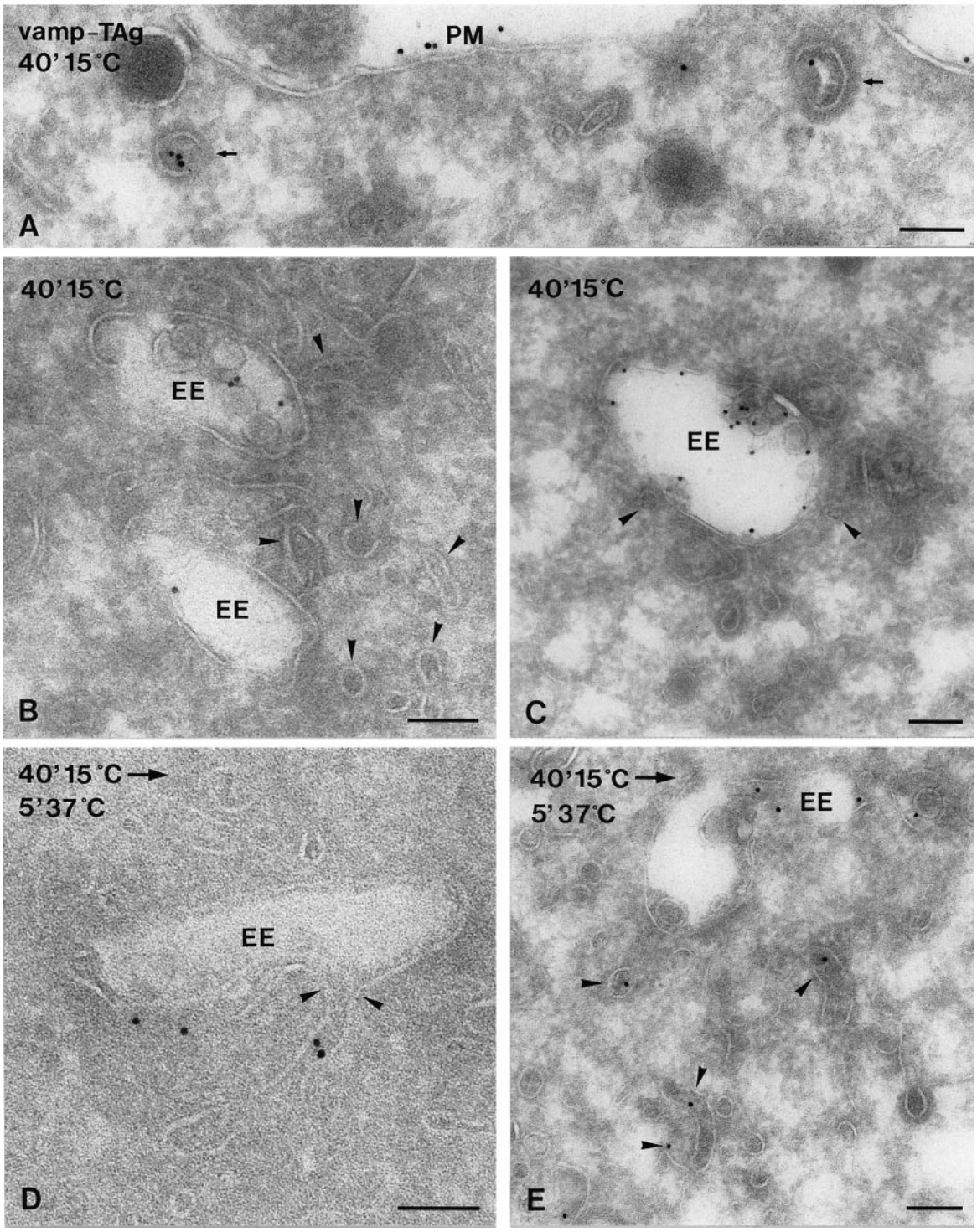

Figure 7. Ultrathin cryosections of VAMP-TAg/N49A PC12 cells. Internalized VAMP-TAg/KT3 antibody complexes were labeled on the sections with rabbit anti-mouse IgG and protein A-gold. Cells were either directly fixed after 40 min at 15°C (A) or first washed to remove plasma membrane-bound antibodies and then fixed (B and C) or first warmed to 37°C before fixation (D and E). After 40 min at 15°C, internalized VAMP-TAg was found in clathrin-coated endocytic vesicles (A, arrows) and the vacuolar domain of EEs (B and C). EE-associated tubules and vesicles were not labeled (B and C, arrowheads). Warming for 5 min to 37°C resulted in the appearance of internalized VAMP-TAg in EE-associated tubules and vesicles (D and E, arrowheads). PM, plasma membrane. Bars, 100 nm.

Table 4. Subcellular distribution of internalized VAMP-TAg/KT3 antibody complexes

Time of rewarming (min)	Primary endocytic vesicles	EEs		LEs	Lysosomes	SLMVs	PM
		Vacuole	Tubules/vesicles				
0	32 ± 1.6	56 ± 1.9	6 ± 1.4	5 ± 1.0	0	0	1 ± 0.7
5	3 ± 0.5	33 ± 1.6	20 ± 2.6	5 ± 1.2	3 ± 0.9	35 ± 0.9	1 ± 0.2
25	7 ± 0.5	16 ± 1.6	22 ± 1.9	5 ± 0.9	7 ± 1.2	42 ± 2.1	1 ± 0.3

VAMP-TAg/KT3 antibody complexes were internalized for 40 min at 15°C, after which plasma membrane (PM)-associated label was washed away, and cells were rewarmed to 37°C. Internalized complexes were visualized on cryosections by immunogold labeling with a rabbit anti-mouse IgG antibody. The numbers represent the mean percentages of total gold particles ± SD.

of EEs to the associated tubules, and that SLMVs are formed by budding from EE tubules.

Finally, we analyzed the morphology of a membrane fraction enriched in SLMV donor compartments (Lichtenstein *et al.*, 1998). The majority of membranes present within this fraction consisted of irregularly shaped, 300- to 400-nm organelles, sometimes with tubular extensions, that contained synaptophysin, VAMP-2, and internalized HRP (Figure 8). Thus, consistent with the idea that EE vacuoles are the 15°C donor compartments for SLMVs, the morphology of the compartments present in the SLMV donor fraction was compatible with that of EE vacuoles in situ.

Because in PC12 cells SLMV formation can also occur directly from the plasma membrane (Schmidt *et al.*, 1997; Shi *et al.* 1998), it was an important point to establish whether the EEs are bona fide intracellular organelles and not invaginations of the plasma membrane. A first indication that EEs are of intracellular origin is the presence of regularly sized, ~70- to 80-nm vesicles in the EE vacuole. These internal vesicles arise by microautophagy, i.e. invagination of small portions of the limiting membrane of the endosomal vacuole, and accumulate in the vacuolar part of maturing endosomes (reviewed by Geuze, 1998). Second, EEs were not stained with the membrane impermeant dye ruthenium red, a marker for plasma membrane-associated structures (Damke *et al.*, 1994). As a positive control for this method, we observed staining of seemingly intracellular clathrin-coated vesicles, which outside the plane of the section by long tubules still were connected to the plasma membrane. Finally, EEs were found positive for the small GTPase rab4, a cytosolic protein that is known to associate with EEs but not the plasma membrane (van der Sluijs *et al.*, 1991, 1992; Daro *et al.*, 1996). Thus, by three different criteria we found no indications that the EE-defined compartments were connected to the plasma membrane.

With our approach we did we not find narrow-necked plasmalemmal invaginations containing synaptophysin and lacking TfR (Schmidt *et al.*, 1997), nor have we been able to identify a pathway of internalization directly from the plasma membrane that morphologically differed from the clathrin-coated pit pathway. We did find clusters of synaptophysin-positive, TfR-negative vesicles near the plasma membrane (Figure 5A), but these vesicles were not loaded with internalized BSA-gold or VAMP-TAg after short incubation times, did not stain for ruthenium red, and were positive for rab3, indicating that these were SLMVs rather

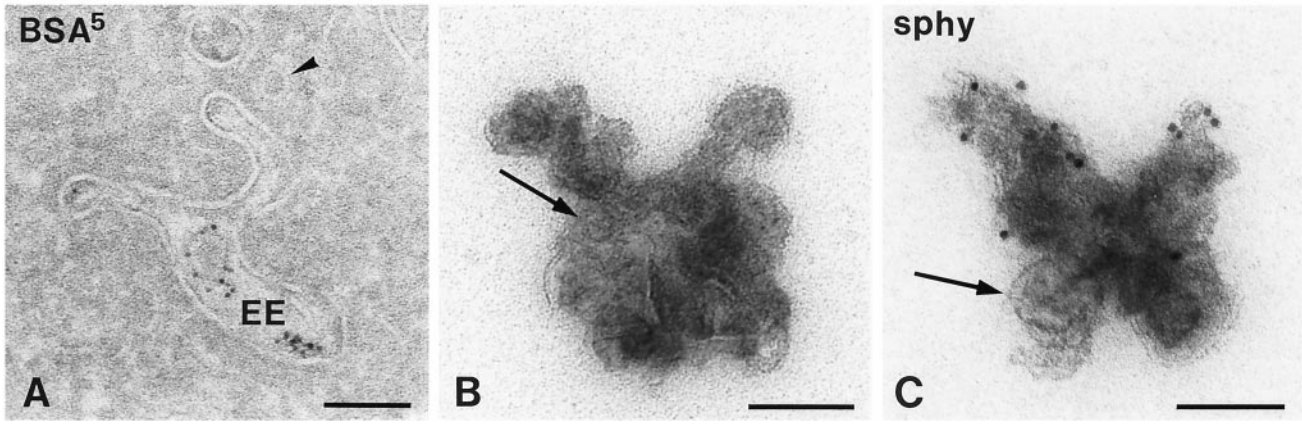

Figure 8. (A) Ultrathin cryosection of a PC12 cell showing a typical EE vacuole with internalized BSA-gold (5-nm gold). (B) Whole-mount image of an isolated SLMV donor compartment. HRP was internalized in VAMP-TAg/N49A PC12 cells for 40 min at 15°C. Cells were fractionated, and isolated SLMV donor compartments were prepared for whole-mount electron microscopy as described in the MATERIALS AND METHODS. (C) SLMV donor compartment immunogold labeled for sphy (10-nm gold). The arrows in B and C indicate globular DAB precipitates indicative of the presence of endocytosed HRP. Bars, 100 nm.

than plasma membrane-associated compartments involved in endocytosis. A prerequisite for SLMV reformation directly from the plasma membrane would be sorting of SLMV proteins and TfR before internalization. Our quantitations in primary endocytic vesicles (Table 3) show a slightly higher level of colocalization of synaptophysin and VAMP-2 than of synaptophysin and the TfR, which indirectly supports a partial sorting of SLMV proteins and the TfR at the plasma membrane. SLMV formation from the plasma membrane might then be mediated by uncoating of a subclass of clathrin-coated vesicles containing high levels of SLMV proteins. Such a scenario would be in agreement with the dependance of this pathway on AP-2, dynamin, and clathrin (Schmidt *et al.*, 1997; Shi *et al.*, 1998).

ACKNOWLEDGMENTS

We are grateful to R. Jahn and A. Hasilik for generously providing antibodies against VAMP-2 and rab3, and cathepsin D, respectively. We thank T. van Rijn, M. Niekerk, and R. Scriwaneck for the excellent preparation of the electron micrographs, V. Oorschot for assisting in the preparation of ultrathin cryosections, and our colleagues in the Department of Cell Biology for their insightful comments. H.d.W. was supported by a grant from the Research Council for Earth and Lifesciences, J.K. and P.v.d.S. were supported by Aard en Levenswetenschappen grant SLW 805-26-183, with financial aid from the Netherlands Organization for Scientific Research, and Y.L. was supported by a fellowship from the Human Frontier Science Program. In addition this work was supported by National Institutes of Health grants NS09878 and DA10154 (to R.B.K.). P.v.d.S. is an investigator of the Royal Netherlands Academy of Arts and Sciences.

REFERENCES

Ayad, N., Hull, M., and Mellman, I. (1997). Mitotic phosphorylation of rab4 prevents binding to a specific receptor on endosome membranes. EMBO J. *16*, 4497–4507.

Bauerfeind, R., Galli, T., and De Camilli, P. (1996). Molecular mechanisms in synaptic vesicle recycling. J. Neurocytol. *25*, 701–715.

Bauerfeind, R., Jelinek, R., and Huttner, W.B. (1995). Synaptotagmin I- and II-deficient PC12 cells exhibit calcium-independent, depolarization-induced neurotransmitter release from synaptic-like microvesicles. FEBS Lett. *364*, 328–334.

Bauerfeind, R., Régnier-Vigouroux, A., Flatmark, T., and Huttner, W.B. (1993). Selective storage of acetylcholine, but not catecholamines, in neuroendocrine synaptic-like microvesicles of early endosomal origin. Neuron *11*, 105–121.

Bean, A.J., and Scheller, R.H. (1997). Better late than never: a role for rabs late in exocytosis. Neuron *19*, 751–754.

Bottger, G., Nagelkerken, B., and van der Sluijs, P. (1996). Rab4 and rab7 define distinct endocytic compartments. J. Biol. Chem. *271*, 29191–29197.

Calakos, N., and Scheller, R.H. (1996). Synaptic vesicle biogenesis, docking, and fusion: a molecular description. Physiol. Rev. *76*, 1–29.

Cameron, P., Mundigl, O., and De Camilli, P. (1993). Traffic of synaptic vesicle proteins in polarized and nonpolarized cells. J. Cell Sci. Suppl. *17*, 93–100.

Cameron, P.L., Südhof, T.C., Jahn, R., and De Camilli, P. (1991). Colocalization of synaptophysin with transferrin receptors: implications of synaptic vesicle biogenesis. J. Cell Biol. *115*, 151–164.

Clift-O'Grady, L., Desnos, C., Lichtenstein, Y., Faúndez, V., Horng, J.-T., and Kelly, R.B. (1998). A method for the reconstitution of synaptic vesicle biogenesis from PC12 cell membranes. Methods *16*, 150–159.

Clift-O'Grady, L., Linstedt, A.D., Lowe, A.W., Grote, E., and Kelly, R.B. (1990). Biogenesis of synaptic vesicle-like structures in a pheochromocytoma cell line PC-12. J. Cell Biol. *110*, 1693–1703.

Damke, H., Baba, T., Warnock, D.E., and Schmid, S.L. (1994). Induction of mutant dynamin specifically blocks endocytic coated vesicle formation. J. Cell Biol. *127*, 915–934.

Daro, E., van der Sluijs, P., Galli, T., and Mellman, I. (1996). Rab4 and cellubrevin define early endosomal populations on the pathway of transferrin receptor recycling. Proc. Natl. Acad. Sci. USA *93*, 9559–9564.

Desnos, C., Clift-O'Grady, L., and Kelly, R.B. (1995). Biogenesis of synaptic vesicles in vitro. J. Cell Biol. *130*, 1041–1049.

Edelmann, L., Hanson, P.I., Chapman, E.R., and Jahn, R. (1995). Synaptobrevin binding to synaptophysin: a potential mechanism for controlling the exocytotic fusion machine. EMBO J. *14*, 224–231.

Faúndez, V., Horng, J.-T., and Kelly, R.B. (1997). ADP ribosylating factor 1 is required for synaptic vesicle budding in PC12 cells. J. Cell Biol. *138*, 505–515.

Faúndez, V., Horng, J.-T., and Kelly, R.B. (1998). A function of AP3 coat complex in synaptic vesicle formation from endosomes. Cell *93*, 423–432.

Fesce, R., Grohovaz, F., Valtorta, F., and Meldolesi, J. (1994). Neurotransmitter release: fusion or "kiss-and-run" Trends Cell Biol. *4*, 1–4.

Geuze, H.J. (1998). The role of endosomes and lysosomes in MHC class II functioning. Immunol. Today *19*, 282–287.

Geuze, H.J., J.W. Slot, Strous, G.J.A.M., Peppard, J., von Figura, K., Hasilik, A., and Schwartz, A.L. (1984). Intracellular receptor sorting during endocytosis: comparative immunoelectron microscopy of multiple receptors in rat liver. Cell *37*, 195–204.

Geuze, H.J., Slot, J.W., van der Ley, P.A., and Scheffer, R.C.T. (1981). Use of colloidal gold particles in double-labeling immunoelectron microscopy on ultrathin frozen sections. J. Cell Biol. *89*, 653–665.

Glickman, J.N., Morton, P.A., Slot, J.W., Stuart, S., and Geuze, H.J. (1996). The biogenesis of the MHC class II compartment in human I-cell disease B lymphoblasts. J. Cell Biol. *132*, 769–785.

Greene, L.A., and Tischler, A.S. (1976). Establishment of a noradrenergic clonal line of rat adrenal pheochromocytoma cells which respond to nerve growth factor. Proc. Natl. Acad. Sci. USA *73*, 2424–2428.

Griffiths, G., Back, R., and Marsh, M. (1989). A quantitative analysis of the endocytic pathway in baby hamster kidney cells. J. Cell Biol. *109*, 2703–2720.

Grote, E., Hao, J.C., Bennett, M.K., and Kelly, R.B. (1995). A targeting signal in VAMP regulating transport to synaptic vesicles. Cell *81*, 581–589.

Grote, E., and Kelly. R.B. (1996). Endocytosis of VAMP is facilitated by a synaptic vesicle targeting signal. J. Cell Biol. *132*, 537–547.

Helenius, A., Mellman, I., Wall, D., and Hubbard, A. (1983). Endosomes. Trends Biochem. Sci. *8*, 245–250.

Heuser, J.E., and Reese, T.S. (1973). Evidence for recycling of synaptic vesicle membrane during transmitter release at the frog neuromuscular junction. J. Cell Biol. *57*, 315–344.

Johnston, P.A., Cameron, P.L., Stukenbrok, H., Jahn, R., De Camilli, P., and Südhof, T.C. (1989). Synaptophysin is targeted to similar microvesicles in CHO and PC12 cells. EMBO J. *8*, 2863–2872.

Kelly, R.B. (1993a). Storage and release of neurotransmitters. Cell *10*(suppl), 43–53.

Kelly, R.B. (1993b). A question of endosomes. Nature *364*, 487–488.

Kleijmeer, M.J., Morkowski, S., Griffith, J.M., Rudensky, A.Y., and Geuze, H.J. (1997). Major histocompatibility complex class II compartments in human and mouse B lymphoblasts represent conventional endocytic compartments. J. Cell Biol. *139*, 639–649.

Klumperman, J., Hille, A., Veenendaal, T., Oorschot, V., Stoorvogel, W., Von Figura, K., and Geuze, H.J. (1993). Differences in the endosomal distributions of the two mannose 6-phosphate receptors. J. Cell Biol. *121*, 997–1010.

Koenig, J.H., and Ikeda, K. (1996). Synaptic vesicles have two distinct recycling pathways. J. Cell Biol. *135*, 797–808.

Lah, J.J., and Burry, R.W. (1993). Synaptophysin has a selective distribution in early endosomes of PC12 cells. J. Neurocytol. *22*, 92–101.

Lichtenstein, Y., Desnos, C., Faúndez, V., Kelly, R.B., and Clift-O'Grady, L. (1998). Vesiculation and sorting from PC12-derived endosomes *in vitro*. Proc. Natl. Acad. Sci. USA *95*, 11223–11228.

Linstedt, A.D., and Kelly, R.B. (1991). Synaptophysin is sorted from endocytotic markers in neuroendocrine PC12 cells but not transfected fibroblasts. Neuron *7*, 309–317.

Liou, W., Geuze, H.J., and Slot, J.W. (1996). Improved structural integrity of cryosections for immunogold labeling. Histochem. Cell Biol. *106*, 41–58.

Llona, I. (1995). Synaptic like microvesicles: do they participate in regulated exocytosis? Neurochem. Int. *27*, 219–226.

Marsh, M., Griffiths, G., Dean, G.E., Mellman, I., and Helenius, A. (1986). Three-dimensional structure of endosomes in BHK-21 cells. Proc. Natl. Acad. Sci. USA *83*, 2899–2903.

Matteoli, M., Takei, K., Cameron, R., Hurlbut, P., Johnston, P.A., Jahn, R., Südhof, T.C., and De Camilli, P. (1991). Association of Rab3A with synaptic vesicles at late stages of the secretory pathway. J. Cell Biol. *115*, 625–633.

Mayor, S., Presley, J.F., and Maxfield, F.R. (1993). Sorting of membrane components from endosomes and subsequent recycling to the cell surface occurs by a bulk flow process. J. Cell Biol. *121*, 1257–1269.

McMahon, H.T., Bolshakov, Y.Y., Janz, R., Hammer, R.E., Siegelbaum, S.A., and Südhof, T.C. (1996). Synaptophysin, a major synaptic vesicle protein, is not essential for neurotransmitter release. Proc. Natl. Acad. Sci. USA *93*, 4760–4764.

Murthy, V.N., and Stevens, C.F. (1998). Synaptic vesicles retain their identity through the endocytic cycle. Nature *392*, 497–501.

Navone, F., Jahn, R., Di Gioia, G., Stukenbrok, H., Greengard, P., and De Camilli, P. (1986). Protein p38: an integral membrane protein specific for small vesicles of neurons and neuroendocrine cells. J. Cell Biol. *103*, 2511–2527.

Régnier-Vigouroux, A., Tooze, S.A., and Huttner, W.B. (1991). Newly synthesized synaptophysin is transported to synaptic-like microvesicles via constitutive secretory vesicles and the plasma membrane. EMBO J. *10*, 3589–3601.

Schmid, S.L., and Smythe, E. (1991). Stage-specific assays for coated pit formation and coated vesicle budding in vitro. J. Cell Biol. *114*, 869–880.

Schmidt, A., Hannah, M.J., and Wieland, W.B. (1997). Synaptic-like microvesicles of neuroendocrine cells originate from a novel compartment that is continuous with the plasma membrane and devoid of transferrin receptor. J. Cell Biol. *137*, 445–458.

Shi,G., Faundez, V., Roos, J., Dell'Angelica, E.C., and Kelly, R.B. (1998). Neuroendocrine synaptic vesicles are formed in vitro by both clathrin-dependent and clathrin-independent pathways. J. Cell Biol. *143*, 947–955.

Slot, J.W., Geuze, H.J., Gigengack, S., Lienhard, G.E., and James, D.E. (1991). Immunolocalization of the insulin regulatable glucose transporter in brown adipose tissue of the rat. J. Cell Biol. *113*, 123–135.

Slot, J.W., Geuze, H.J., and Weerkamp, A.H. (1988). Localization of macromolecular components by application of the immunogold technique on cryosectioned bacteria. Methods Microbiol. *20*, 211–236.

Stoorvogel, W., Oorschot, V., and Geuze, H.J. (1996). A novel class of clathrin-coated vesicles budding from endosomes. J. Cell Biol. *132*, 21–33.

Takei, K., Mundigl, O., Daniell, L., and De Camilli, P. (1996). The synaptic vesicle cycle: a single vesicle budding step involving clathrin and dynamin. J. Cell Biol. *133*, 1237–1250.

Trimble, W.S., Cowan, D.M., and Scheller, R.H. (1988). VAMP-1: a synaptic vesicle-associated integral membrane protein. Proc. Natl. Acad. Sci. USA *85*, 4538–4542.

van der Sluijs, P., Hull, M., Webster, A.P., Goud, B., and Mellman, I. (1992). The small GTP-binding protein rab4 controls an early sorting event on the endocytic pathway. Cell *70*, 729–740.

van der Sluijs, P., Hull, M., Zahraoui, A., Tavitian, A., Goud, B., and Mellman, I. (1991). The small GTP-binding protein rab4 is associated with early endosomes. Proc. Natl. Acad. Sci. USA *88*, 6313–6317.

White, S., Miller, K., Hopkins, C.R., and Trowbridge, L.S. (1992). Monoclonal antibodies against the defined epitopes of the human transferrin receptor cytoplasmic tail. Biochim. Biophys. Acta *1136*, 28–34.

Wiedenmann, B., and Franke, W.W. (1985). Identification and localization of synaptophysin, an integral membrane glycoprotein of M_r 38,000 characteristic of presynaptic vesicles. Cell *41*, 1017–1028.

Wiedenmann, B., Rehm, H., Knierim, M., and Becker, C.-M. (1988). Fractionation of synaptophysin-containing vesicles from rat brain and cultured PC12 pheochromocytoma cells. FEBS Lett. *240*, 71–77.